Power Flow and Dynamic Modeling of Static Var Sources Based on a Generic Description Framework

Yujun Zhou
School of Electrical Engineering
Shandong University
Jinan, China
202414666@mail.sdu.edu.cn

Dongbao Lv
School of Electrical Engineering
Shandong University
Jinan, China
dlv@mail.sdu.edu.cn

Jiawen Cao
School of Electrical Engineering
Shandong University
Jinan, China
caojiawen@mail.sdu.edu.cn

Changgang Li*
School of Electrical Engineering
Shandong University
Jinan, China
lichgang@sdu.edu.cn

***Abstract*—This paper proposes techniques for power flow and dynamic modeling of static var (SV) sources. Firstly, a generic modeling description framework is established, in which an equivalent reactive power injection at the nominal bus voltage and a voltage-response function jointly describe characteristics of SV sources. Based on this framework, an improved power-flow algorithm is developed that explicitly enforces the reactive capability limits of SV sources. A generic dynamic model is further constructed with a unified control model and a current-source interface, which can emulate both static var compensator (SVC) and static var generator (SVG) dynamic behavior. The proposed power-flow algorithm and dynamic model of SV sources have been implemented in the open-source simulation toolkit STEPS through an object-oriented SOURCE/SV_SOURCE class and the SGFLSVS0 dynamic model. Dynamic simulations on a single machine infinite bus (SMIB) system not only verify the accuracy and computational efficiency of the proposed dynamic model but also reveal the mechanisms responsible for the different magnitudes of transient overvoltages produced by various types of SV sources. Comparative power-flow studies on a provincial 132-bus system in China against PSS/E demonstrate the accuracy of the proposed power-flow algorithm and dynamic simulations on this system confirm that SV sources can effectively support the stable operation of renewable energy plants.**

***Index Terms*—static var source modeling, generic description framework, power flow algorithm, generic dynamic model, open-source toolkit, stability support**

I. Introduction

With the increasing penetration of grid-connected wind and photovoltaic plants and long-distance power transfers, many transmission corridors and renewable collection networks operate with low short-circuit strength and tight reactive power margins, making bus voltages more sensitive to disturbances [1]. Under such conditions, insufficient reactive support may cause voltage sags and even disconnection of renewable generation units, thus threatening the stable operation of renewable energy plants as well as the bulk power system [2], [3]. To comply with modern grid codes and safeguard plant-level stability, renewable power plants are therefore often equipped with static var (SV) sources at their points of common coupling to provide rapid voltage support and reinforce the phase-locking capability of converter-based units [4]. These trends motivate accurate and efficient SV models for both steady-state power-flow analysis and electromechanical transient studies.

In most existing tools, static var compensator (SVC) and static var generator (SVG) are modeled separately as variable shunt susceptances and current-controlled devices according to their physical implementation [5]–[7]. In conventional power-flow formulations, capability constraints are imposed directly on the reactive power output. Such a treatment does not explicitly expose the true limiting quantities, the admissible susceptance range of SVCs and the current limit of SVGs—and may distort the effective capability boundaries when the bus voltage deviates from its nominal value [6]–[8]. For dynamic simulations, SVC and SVG models are often developed with similar control structures but different interface variables and parameter sets, leading to duplicated modeling efforts and inconsistencies between device types [5], [7]. Moreover, the corresponding implementations in commercial software are typically closed-source, which limits their transparency and extensibility for research.

The main contributions of this paper are as follows: (1)A generic description framework is proposed, which can represent SV sources in a unified manner. (2)An improved power-flow algorithm is developed, which is suitable for modeling reactive power sources within the above framework. (3)A generic dynamic model of SV sources is proposed, which can emulate both SVC and SVG dynamic behavior in a single model. (4)The proposed algorithms and models are implemented in STEPS and publicly released as open-source code. Comparative studies against PSS/E and MATLAB verify the accuracy of the models and demonstrate the effectiveness of SV sources in supporting renewable energy integration.

This work is supported by Smart Grid-National Science and Technology Major Project (2024ZD0802900).

979-8-3315-8138-1

II. Generic Description Framework of SV Sources

A. Two Commonly Used Static Var Sources

Two commonly used SV sources are SVC and SVG.

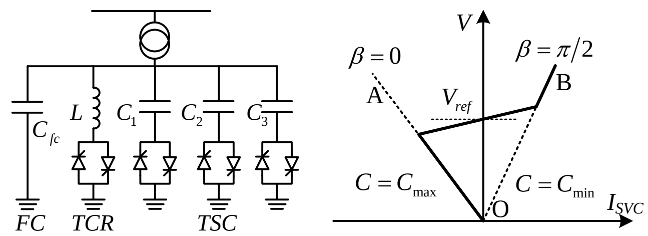

(a) (b)

Fig. 1. SVC device. (a)single-line diagram. (b)V–I characteristic.

$$B_{\mathrm{SVC}} = \omega C - \frac{2\beta - \sin 2\beta}{\pi \, \omega L}. \tag{1}$$

The SVC is a susceptance-controlled SV source. As shown in Fig. 1(a), the SVC consists of a thyristor-controlled reactor (TCR), thyristor-switched capacitors (TSCs), and filter capacitors (FCs). By continuously tuning the conduction angle β of TCR in coordination with full-on/full-off switching of TSC capacitors, the equivalent susceptance can be controlled continuously. The SVC equivalent susceptance is given by (1) [9]. When the conduction angle is zero and the TSC capacitor bank is full-on, B_{SVC} is the maximum value, corresponding to the OA branch of the V–I characteristic in Fig. 1(b). The minimum B_{SVC} value corresponds to branch OB.

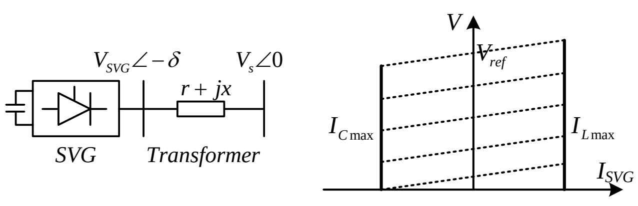

(a) (b)

Fig. 2. SVG device. (a)single-line diagram. (b)V–I characteristic.

$$I_{\mathrm{SVG\_q}} \;=\; \frac{V_s}{2r}\,\sin 2\delta. \tag{2}$$

The SVG is a current-controlled SV source. As shown in Fig. 2(a), the SVG is essentially a three-phase bridge inverter that is interfaced to the grid via a step-up transformer. By adjusting the PWM modulation index and the firing angle of the inverter, the amplitude and phase of the inverter output voltage are controlled, thereby regulating the injected current. SVG reactive injected current is given by (2) [9]. From the V–I characteristic in Fig. 2(b), SVG operates under a maximum current-output limit, and compared with SVC, exhibits a wider operating range.

According to the above description, SV sources adjust reactive output indirectly—either by varying the susceptance or by controlling the injected current—and their operating range is constrained by the maximum current or the admissible susceptance range. However, the conventional description framework of reactive power sources imposes constraints only on reactive power output. Such a framework fails to reflect both the physical operating mechanisms and the current- and susceptance-limited characteristics of SV sources.

This motivates a description framework that can more generically characterize the operating behavior and capability limits of all types of reactive power sources.

B. Generic $\tilde{Q}$-$f(V^*)$ Framework

Including conventional sources, reactive power sources can be classified by their primary controlled variable into power-controlled (e.g. synchronous generator, SG), current-controlled (e.g. SVG), and susceptance-controlled (e.g. SVC) types, and their reactive power output characteristics are given by (3).

$$\begin{cases} Q_{\mathrm{out,SG}} = Q \cdot 1 \\ Q_{\mathrm{out,SVG}} = I\,V_n \cdot V^* \\ Q_{\mathrm{out,SVC}} = B\,V_n^2 \cdot V^{*2} \end{cases} \tag{3}$$

Reactive power output characteristics of reactive power sources are determined by two components: current reactive power capability and its voltage-response characteristic. Accordingly, a generic description framework is proposed with two core descriptors in (4)—the equivalent reactive injection in Mvar at nominal voltage $\tilde{Q}$ ($\triangleq Q_{\mathrm{out}}\big|_{V=V_n}$) and the voltage-response function $f(V^*)$ to describe above two characteristics.

$$Q_{\mathrm{out}} = \tilde{Q} \cdot f(V^*) \tag{4}$$

According to the definition, $\tilde{Q}$ is determined by the device's own operating parameters and is independent of the present system voltage. Device-level constraints expressed in different quantities—such as $[\,Q_{\min},\, Q_{\max}\,]$, $[\,B_{\min},\, B_{\max}\,]$ and $|I| \leq I_{\max}$ can all be mapped to an equivalent range $[\,\tilde{Q}_{\min},\, \tilde{Q}_{\max}\,]$. Consequently, device capability boundaries are uniformly measured by $\tilde{Q}$, which not only enables direct comparison across different types of reactive power sources but also facilitates modeling and reactive power planning in power systems.

The function $f(V^*)$ is introduced to characterize a reactive power source's voltage response mechanism. V^* is the per-unit voltage referenced to the nominal voltage. For power-controlled devices, the reactive output is independent of voltage. For current-controlled devices, the reactive output is proportional to the voltage. For susceptance-controlled devices, the reactive output is proportional to the square of the voltage. Accordingly, $f(V^*)$ provides a direct description of "how the reactive power varies with voltage."

Within the above generic $\tilde{Q}$-$f(V^*)$ framework, it suffices to specify the admissible range $[\,\tilde{Q}_{\min},\, \tilde{Q}_{\max}\,]$ and according to the device type, choose an appropriate $f(V^*)$ to clearly characterize the capability boundaries and voltage-response characteristics of different reactive power sources.

979-8-3315-8138-1

According to (3), the $\tilde{Q}$ and f(V^*) specifications for different reactive power source types can be summarized in Table I.

TABLE I
PARAMETER IDENTIFICATION FOR THE $\tilde{Q}$-$f(V^*)$ FRAMEWORK

Device Type	$\tilde{Q}$	$f(V^*)$
SG	Q	1
SVG	$I\,V_n$	V^*
SVC	$B\,V_n^2$	$(V^*)^2$

III. POWER FLOW AND GENERIC DYNAMIC MODELING BASED ON $\tilde{Q}$-$f(V^*)$ FRAMEWORK

A. Power Flow Algorithm

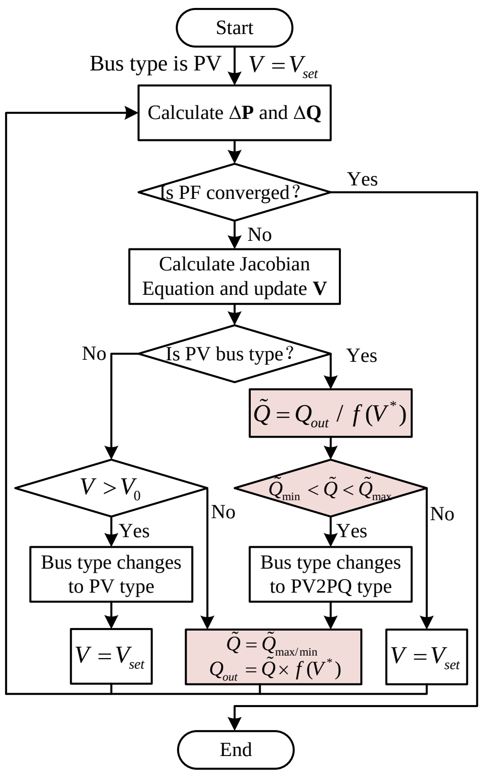

Fig. 3. Power flow algorithm of PV bus connected with SV sources.

To ensure that SV sources exhibit their true capability limits in power flow calculation, it is necessary to modify the conventional power flow algorithm. Within the generic framework, the operating range of SV sources is specified by $[\tilde{Q}_{\min}, \tilde{Q}_{\max}]$. Therefore, a $\tilde{Q}$-limit handling step is incorporated into the conventional Newton method: map the requested Q_{out} to the $\tilde{Q}$-domain for limit checking and clamping, and then map it back to the physical reactive output to participate in the iteration.

Fig. 3 illustrates the special treatment of PV type bus connected with SV sources in power flow calculation. After each update of the voltage vector, we first verify whether the device can provide sufficient reactive support. Rather than checking the PV bus reactive output directly, the requested reactive power output is mapped to the $\tilde{Q}$-domain as $\tilde{Q} = Q_{\text{out,PV}}/f(V^*)$ and compared with the admissible range $[\tilde{Q}_{\min}, \tilde{Q}_{\max}]$. If a limit is violated, the bus type switches from PV to PQ, the $\tilde{Q}$ is clamped at the boundary; otherwise, the bus remains PV with V equal to V_{set}.

It is worth noting that when $f(V^*) = 1$, the PV bus constraint check degenerates to the conventional power flow method that enforces limits directly on reactive power output, underscoring the greater generality of the proposed power flow algorithm.

B. Generic Dynamic Model

TABLE II
DYNAMIC-MODEL STRUCTURAL AND FUNCTIONAL COMPARISON FOR SV SOURCES

Function	SVC	SVG
Voltage Measurement	✓	✓
Voltage Regulation	✓	✓
Slow Vref Control	✓	✓
Droop Control	✓	✓
Interface	susceptance	reactive current
Operating Bounds	$[B_{\min}, B_{\max}]$	$[I_{\min}, I_{\max}]$

Table II summarizes the structural and functional similarities and differences between the SVC and SVG dynamic models. The two are partially similar in their control models; the main distinctions lie in how the operating boundaries are expressed and in the grid interface—SVC uses a shunt susceptance interface, whereas SVG uses a reactive current interface. Hence, by employing the generic $\tilde{Q}$-$f(V^*)$ framework for SV sources, the two models can be merged into a single generic model.

As illustrated in Fig. 4, in the process of model combination, both devices are abstracted by a unified control model that regulates an equivalent capability $\tilde{Q}_{svs}$, with limit handling performed over the interval $[\tilde{Q}_{\min}, \tilde{Q}_{\max}]$. The resulting output is then mapped to the current–source interface via the voltage–response function $f(V^*)$.

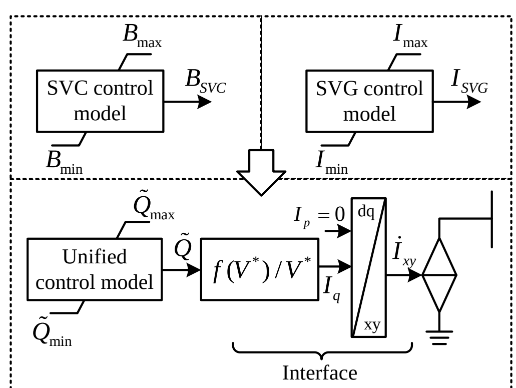

Fig. 4. Generic dynamic model formulation of SV sources.

979-8-3315-8138-1

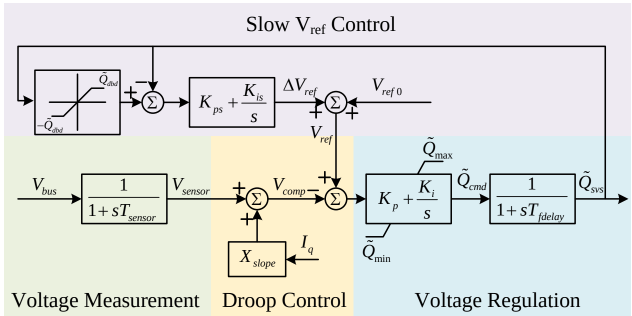

Fig. 5. Structure of SV sources unified control model.

The structure of SV sources unified control model is shown in Fig. 5. In summary, the generic dynamic model of SV sources includes:

- Voltage measurement model: models the delay of voltage measurement and filtering.
- Voltage regulation model: adjusts $\tilde{Q}$ based on the voltage error. $\tilde{Q}$ is clamped within $[\tilde{Q}_{\min}, \tilde{Q}_{\max}]$.
- Slow Vref control model: ensures that the steady-state output remains within the control bandwidth.
- Droop control model: models the droop characteristic of SV sources.
- Grid interface model: is emulated as a current source: active and reactive currents are computed as (5) and then apply a reference frame (dq–xy) transformation.

$$\begin{cases} I_{\mathrm{p}} = 0 \\ I_{\mathrm{q}} = \tilde{Q} \cdot f(V^{*}) / V^{*} \end{cases} \tag{5}$$

IV. Model Implementation And Case Study

A. Model Implementation in STEPS

The power flow algorithm and dynamic models of SV sources based on the generic framework are implemented in the open-source Simulation Toolkit for Electrical Power Systems (STEPS) [10]. STEPS adopts an object-oriented design for device modeling. The inheritance relationships between the devices are shown in Fig. 6.

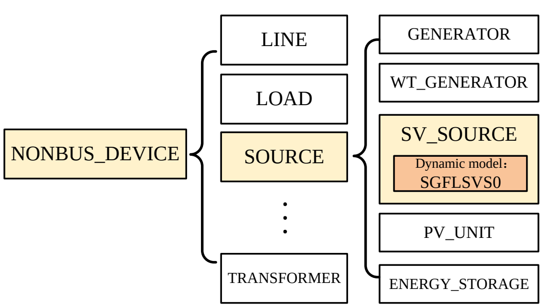

Fig. 6. Devices class inheritance hierarchy in STEPS.

Unlike PSS/E, in which SVC and SVG are separately implemented as SWITCHED SHUNT and FACTS devices, STEPS implements SV sources through a unified class, `SV_SOURCE`. This class inherits from the `SOURCE` base class and shares the same input format as other source types. Moreover, the proposed generic dynamic model is encapsulated within `SV_SOURCE`, named `SGFLSVS0`.

Finally, the proposed model is open-sourced and available at https://github.com/changgang/steps.

B. A SMIB Test Case

To evaluate the dynamic accuracy and simulation efficiency of the proposed dynamic model, comparative simulations against phasor models and electromagnetic transient (EMT) models are conducted in a single machine infinite bus (SMIB) system, as shown in Fig. 7. Specifically, the dynamic behaviors of the proposed model, operating as SVC and SVG, are emulated through the developed SGFLSVS0 model in STEPS, whereas phasor models employ the built-in SVSMO1 and SVSMO3 models in PSS/E and EMT models are implemented in MATLAB. The magnitude of the grid voltage is reduced to 0.7 pu at 3.0s and returns to 1.0 pu at 6.0s.

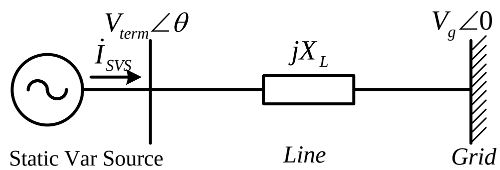

Fig. 7. SMIB system.

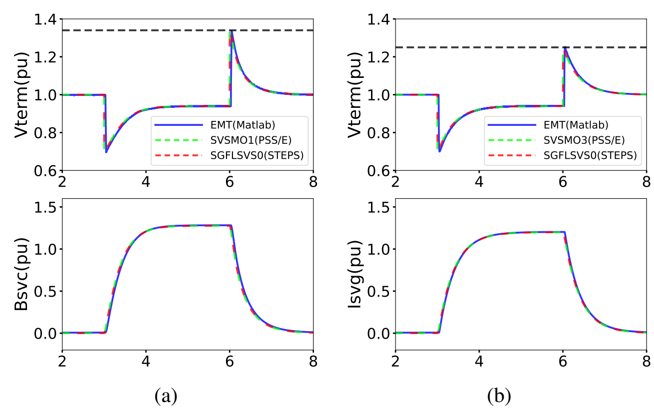

Fig. 8. Comparative dynamic responses among the SGFLSVS0 model, PSS/E phasor models, and EMT models. (a)SVC operation. (b)SVG operation.

As shown in Fig. 8, compared with PSS/E models, simulation errors do not exceed 0.01% and 0.02% in both SVC and SVG operations. In a 10-second simulation, the proposed model completed in 2.3s, while the EMT model required 25.8s. The simulation efficiency is improved by 11.22 times. Due to the droop control, during the grid voltage sag, the SVC and SVG cannot restore the bus voltage to its initial level. When the voltage recovers to 1.0 pu at 6.0s, the SVC exhibits a larger transient overvoltage than the SVG. This is because, at the disturbance instant, the SVC's shunt susceptance cannot change instantaneously. When the voltage steps up, a fixed instantaneous admittance injects more reactive power, since $Q = V^2 B$; this yields a larger reactive burst than a SVG under current control, and thus a larger transient overvoltage.

979-8-3315-8138-1

C. A Provincial 132-Bus System of China Test Case

To validate the accuracy of the proposed power-flow algorithm, comparative studies between STEPS and PSS/E are performed on a provincial 132-bus system of China, as shown in Fig. 9. SVCs are placed at buses 1 and 2, with voltage setpoints of 1.00 pu, and their $\tilde{Q}$ ranges are set to $[-120\,\mathrm{Mvar}, 120\,\mathrm{Mvar}]$. SVGs are installed at buses 3 and 4 with voltage setpoints of 1.00 pu, each configured with a $\tilde{Q}$ range of $[-100\,\mathrm{Mvar}, 100\,\mathrm{Mvar}]$. In PSS/E, the SVCs and SVGs were represented using the built-in SWITCHED SHUNT and FACTS devices, with parameters matched to the STEPS configuration.

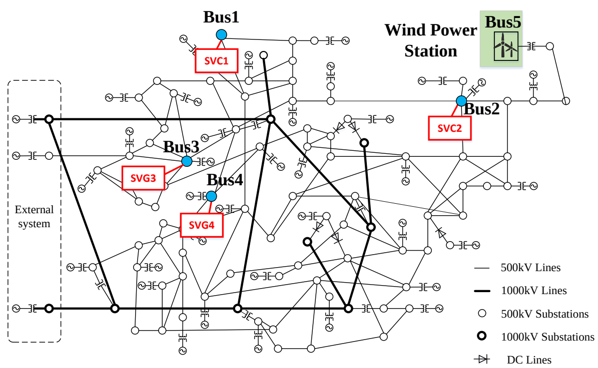

Fig. 9. Topology diagram of the provincial system of China.

TABLE III
POWER FLOW RESULT TABLE

Device	PSS/E		STEPS		
	Q_{MVar}	V_{pu}	Q_{MVar}	V_{pu}	$\tilde{Q}$
SVC1	114.733	1.0000	114.733	1.0000	114.733
SVC2	119.817	0.9992	119.817	0.9992	120.000
SVG3	93.669	1.0000	93.669	1.0000	93.669
SVG4	99.870	0.9987	99.869	0.9987	100.000
iter count	9		9		

Table III shows the power flow results from PSS/E and STEPS. The two solutions differ only marginally, confirming the accuracy of the proposed power-flow algorithm. With a convergence tolerance set to 0.01 MW/Mvar, both solutions converged in 9 iterations, indicating that the proposed algorithm's convergence performance is on par with that of commercial power-flow solvers. It should be noted that the voltages at buses 2 and 4 cannot be maintained at their setpoints, because the SV sources connected at these buses lack sufficient reactive capacity and the $\tilde{Q}$ is clamped at $\tilde{Q}_{\max}$.

Fig. 10 shows the response of the wind power station at bus 5 to a three-phase short-circuit before and after installing a SVG. With the SVG in service, the terminal voltage recovers above 0.9 pu earlier—advanced from 1.596 s to 1.300 s—demonstrating a clear voltage-support capability. In addition, the SVG reduces the maximum phase difference between the PLL output and the terminal-voltage angle from 31.86° to 22.15°, indicating enhanced phase locking of the renewable unit provided by the SV sources.

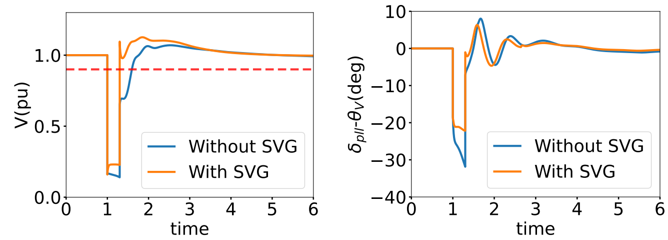

(a) (b)

Fig. 10. Three-phase fault responses of wind power station at bus 5 with and without SVG. (a)terminal voltage response. (b)PLL phase error $\delta_{\mathrm{PLL}} - \theta_V$ response.

V. CONCLUSION

In this work, SV sources are recast into a generic $\tilde{Q}$–$f(V^*)$ framework that is applicable to power-, susceptance- and current-controlled reactive sources. Based on this framework, an improved power-flow algorithm is devised that enforces capability limits directly in the $\tilde{Q}$ domain, and a generic electromechanical-transient model is developed to emulate both SVC and SVG behavior. The framework is implemented in an open-source simulation platform STEPS and validated by comparison with commercial tools. In a SMIB test system, the dynamic simulation errors relative to the phasor model built in PSS/E are all below 0.02%. Compared with EMT models built in MATLAB, the simulation efficiency is improved 11.22 times. In a provincial 132-bus system of China, power-flow results match PSS/E with identical terminal voltages (to three decimal places). The provincial case study further illustrates that SV sources can effectively enhance voltage recovery and phase-locking performance of renewable energy plants.

REFERENCES

[1] F. Arraño-Vargas, Z. Shen, S. Jiang, J. Fletcher, and G. Konstantinou, "Challenges and mitigation measures in power systems with high share of renewables—the Australian experience," *Energies*, vol. 15, no. 2, p. 429, Jan. 2022.

[2] R. Sakipour and H. Abdi, "Voltage stability improvement of wind farms by self-correcting static volt-ampere reactive compensator and energy storage," *Int. J. Electr. Power Energy Syst.*, vol. 140, 2022, no. 108082.

[3] J. Qi, W. Zhao, and X. Bian, "Comparative study of SVC and STATCOM reactive power compensation for prosumer microgrids with DFIG based wind farm integration," *IEEE Access*, vol. 8, pp. 209878–209885, 2020.

[4] F. H. Gandoman, A. Ahmadi, A. M. Sharaf, P. Siano, J. Pou, B. Hredzak, and V. G. Agelidis, "Review of FACTS technologies and applications for power quality in smart grids with renewable energy systems," *Renew. Sustain. Energy Rev.*, vol. 82, pp. 502–514, Feb. 2018.

[5] IEEE Special Stability Controls Working Group, "Static var compensator models for power flow and dynamic performance simulation," *IEEE Trans. Power Syst.*, vol. 9, no. 1, pp. 229–240, Feb. 1994.

[6] E. Acha and B. Kazemtabrizi, "A new STATCOM model for power flows using the Newton–Raphson method," *IEEE Trans. Power Syst.*, vol. 28, no. 3, pp. 2455–2465, Aug. 2013.

[7] P. Pourbeik et al., "Generic model structures for simulating static var systems in power system studies—A WECC task force effort," *IEEE Trans. Power Syst.*, vol. 27, no. 3, pp. 1618–1627, Aug. 2012.

[8] H. Ambriz-Perez, E. Acha, and C. R. Fuerte-Esquivel, "Advanced SVC models for Newton-Raphson load flow and Newton optimal power flow studies," *IEEE Trans. Power Syst.*, vol. 15, no. 1, pp. 129-136, Feb. 2000.

[9] X. Wang, Y. Song, and M. Irving, *Modern Power Systems Analysis*. Power electronics and power systems, Springer US, 2010.

[10] C. Li, Y. Wu, H. Zhang, H. Ye, Y. Liu, and Y. Liu, "STEPS: A portable dynamic simulation toolkit for electrical power system studies," *IEEE Trans. Power Syst.*, vol. 36, no. 4, pp. 3216–3226, Jul. 2021.

979-8-3315-8138-1